A machine vision system using circular autoregressive models for rapid recognition of salmonella typhimurium

O. Trujillo*, C. L. Griffis**, Y. Li., and M. F. Slavik.
otrujil@uark.edu, clg@uark.edu, yanbinli@uark.edu, mslavik@uark.edu

Abstract

The objective of this research was to develop a machine vision system using image processing and statistical modeling techniques to identify and enumerate bacteria on slides containing Salmonella typhimurium. Pictures of bacterial cells were acquired with a CCD camera attached to a motorized fluorescence microscope. A shape boundary modeling technique, based on the use of circular autoregressive model parameters, was used. A feature weighting classifier was trained with ten images belonging to each shape class (rod shape and circle shape). In order to enhance the discrimination of circular shapes, a size range was added to the recognition algorithm. Experimental results showed that the model parameters could be used as descriptors of shape boundaries detected in digitized binary images of bacterial cells. The introduction of the rotated coordinate method and the circular size restriction, reduced the differences between automated and manual recognition/enumeration from 7% to less than 1%. The computer analyzed each image in approximately 5 s (a total of 2 h including sample preparation), while the bacteriologist spent an average of 1 min for each image.

Keywords

Bacteria detection, fluorescence microscopy, machine vision, image analysis, and pattern recognition.

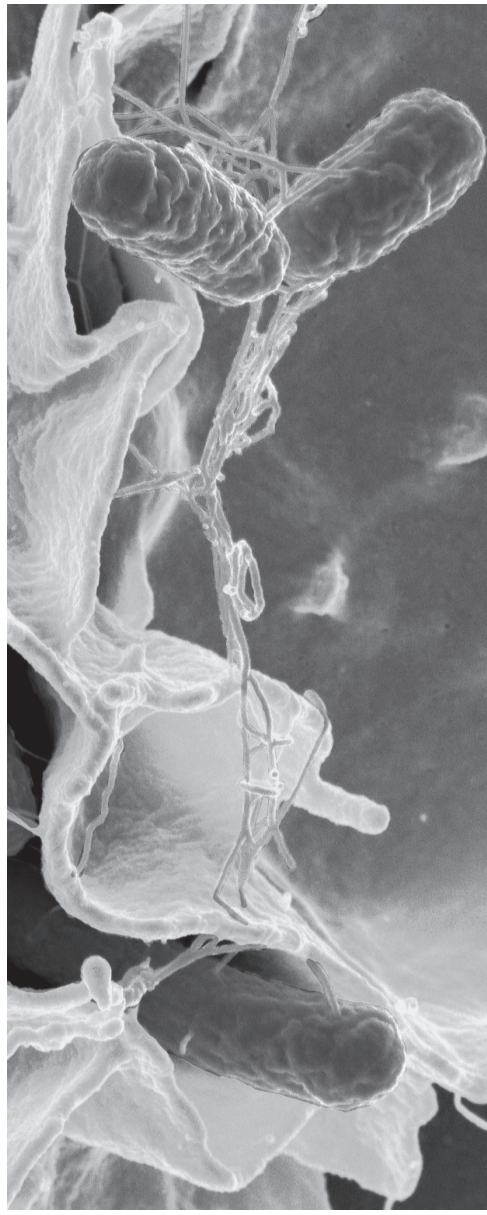

Recibido: 6 de octubre de 2011
Aprobado: 25 de febrero de 2012

*Student ASAE member University of Arkansas, otrujil@uark.edu
** ASAE member University of Arkansas, USA.

Introduction

In a machine vision system, two key elements are considered: image sensing (including optics) and image analysis. A computerized microscope, including motorized stages, and a CCD camera with optical filters can be used as the image sensing equipment. In addition, image-analysis techniques such as binary image dilation/erosion, image segmentation, boundary detection, centroid determination, distance measurements, and image feature extraction can work effectively with pattern recognition techniques. A mathematical representation of an object's shape can be obtained with the use of a statistical signal modeling technique called circular autoregressive (CAR) modeling. The CAR model can be used to express a polygonal approximation of an object boundary as a linear combination of sequential boundary samples plus an error term. With appropriate boundary sampling, functions of the model parameters are invariant to orientation, translation, and scaling of the boundary, and thus, they can be used as shape descriptors of boundaries detected in digitized images of objects such as bacterial cells. In this research, the CAR model for two-dimensional convex shape description of *Salmonella* cells, following the approach of Kashyap and Chellappa (1981), was used. The CAR models have been used for military target identification (Paulik *et al*., 1992), medical imaging (Chen *et al*., 1999), industrial parts identification (Dubois and Glanz., 1986), and food classification (Ghazanfari and Irudayaraj, 1996).

Another important topic in machine vision, especially in the robotic vision area, is the classification of objects in an image. The introduction of machine vision in industrial settings, particularly in the food industry, has become widely utilized (Hand and McCarthy, 2000). In order to decide which shapes are recognized in an image, a minimum distance classifier, known as the feature weighting (FW) method (Dubois and Glanz, 1986), can be used. The FW classifier can be trained with images belonging to each shape class (rod shape and circle shape, in this research).

The purpose of this research was to investigate a method for rapid recognition and enumeration of *Salmonella typhimurium* by the use of a machine vision system. Recognition experiments were performed on samples containing *Salmonella typhimurium* from chicken carcass wash water in order to study the shape discrimination capabilities of the CAR model parameters in conjunction with the Feature Weighting classifier (FW) with and without rotated coordinates (FWR). A second size restriction condition was added to enhance the discrimination of circular shapes. The recognition and enumeration performance of the computer-based system was compared against the visual microscopic count of a trained bacteriologist.

Materials And Methods

Sample preparation

Salmonella typhimurium (ATCC 14028) was grown by placing 10 ml of bacterial suspension in 5 ml of BHI broth (Brain Heart Infusion, Remel, Lenexa, KS) and then incubating for 18 to 24 h at 37 °C. Subsequently, the broth was diluted by 1:10 serial dilutions with PBS at pH 7.4 (Peptone Buffered Saline, Remel, Lenexa, KS). One milliliter of the 10^{-4} dilution, with approximately 1 x 10^5 cfu/ml of *Salmonella* cells, was added to 50 ml of 1-micron anti-*Salmonella* coated beads in an Eppendorf tube. The sample was mixed by rocking it on a Coulter Blood Mixer for 10 min at room temperature. Once the 10-min period was ended, 2 ml (0.5 mg/ml) of fluorescein isothiocyanate (FITC) tagged goat anti-*Salmonella* polyclonal antibody (lot# VB056, Kirkegaard & Perry Laboratories, Inc., Gaithersburg, MD) was added to the sample and the mixture rocked for an additional 30 min. The Eppendorf tube was placed in a magnetic separator rack for 3 min to concentrate the *Salmonella* captured by the magnetic beads onto the side of the tube. Both the supernatant and the remaining liquid in the tube's cap were aspirated and discarded. The Eppendorf tube was removed from the magnetic separator and the magnetic pellet was re-suspended by adding 1 ml of PBS solution containing

0.5% of BSA (Bovine Serum Albumin, St. Louis, MO). The suspension was shaken briefly and placed again in the magnetic separator for 3 min.

After the pellet was washed three times, the supernatant was discarded and a final re-suspension with 1 ml of PBS/BSA (5%) was performed. The final suspension was withdrawn with a sterilized syringe and then filtered through a polycarbonate membrane placed in a filter holder. The membrane filter (0.2 m, 13 mm diameter, Osmonics, Livermore, CA) was placed with the shiny side up on the holder and then moistened with a drop of PBS/BSA solution. The holder was assembled and tightened with the provided ring. After the syringe and the holder were joined, the suspension was forced to pass through the membrane leaving the beads with the captured *Salmonella* on the membrane's surface. Finally, the filter was removed from the holder and placed on a glass slide with small forceps. A drop of mounting fluid (VMRD, Inc., Pullman, WA) was poured on the membrane and a cover slip was placed over it. The slide could then be stored at 4°C in the dark if not used immediately. Using a mounting liquid with a pH close to 9.0 was critical to minimize fluorescence fading.

Implementation of the shape recognition algorithm

A cellular shape recognition algorithm was used to train the computer in the recognition of *Salmonella typhymurium*. A detailed description of the equipment used in this investigation can be found in Trujillo, *et. al.*, (2001). The purpose of each of the different algorithms described here is to transform a video image of a *Salmonella* cell into a set of shape descriptors. This transformation requires acquisition of the image, application of image processing techniques such as segmentation, detection of boundary points, centroid calculation, determination of the radius vector, calculation of model parameters, extraction of the feature vector, and pattern recognition. A summary of the necessary steps for differentiating *Salmonella* cells from other particles such as debris is shown in Figure 1 and fully described in the next sections.

Figure 1. Steps for the recognition of *Salmonella* cells. (A) Image Acquisition and Flatten Filter. (B) Segmentation. (C) Searching for first boundary pixel, boundary follower, and centroid determination. (D) Selection of equally spaced boundary points. (E) Creation of vector with sampled radius distances. (F) Calculation of model parameters and creation of feature vector. (G) Class shape discrimination and decision rule.

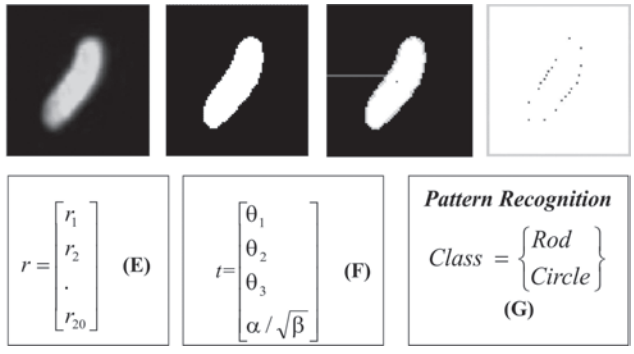

In this research, *Salmonella* cells were classified by the use of circular autoregressive (CAR) model parameters as a representation of the shape of boundaries of digitized images of the bacteria. The CAR model is used to represent *Salmonella*'s two-dimensional closed contour with a particular form of parametric equation. This approach was chosen not only because it is fast and invariant to size and position of the observed object, but also because it has shown good results in recognizing visible portions of *Salmonella* shapes, another problem limiting previous investigations (Huang *et al.*, 1999).

A given boundary can be represented by a one-dimensional radii sequence, $\{r(k)\ \ 1 \le k \le N\}$, which is composed of the radial distances of N marked-off boundary points from the centroid of the bacteria's shape. In addition, the radius vector lengths are a function of the angle of projection $\phi = t2\pi / N$, where $t = 1,\ldots, N$. Figure 2 illustrates this boundary representation with mathematical terms. As Figure 3 shows, the ordered set of k boundary points can also be expressed as a time series $r(k)$, with parameter k describing the position of a radius vector in equal angular increments from the starting point. For instance, $r(1)=r(2p/N)$ and $r(20)=r(2p)$. In order to ensure that the $r(k)$ function is single valued,

Figure 2. Mathematical boundary representation.

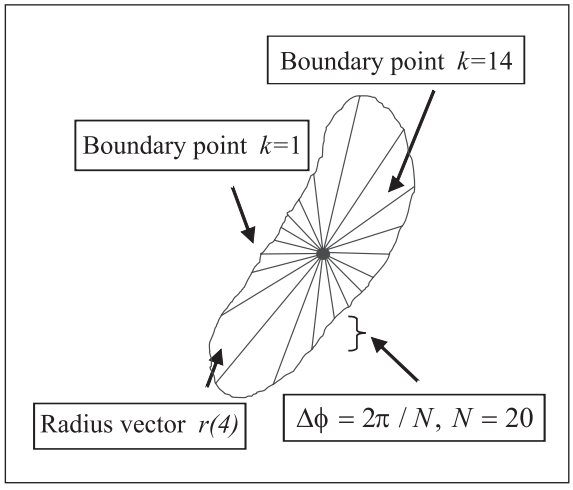

Figure 3. Plot of radii distances vs. sampled boundary points

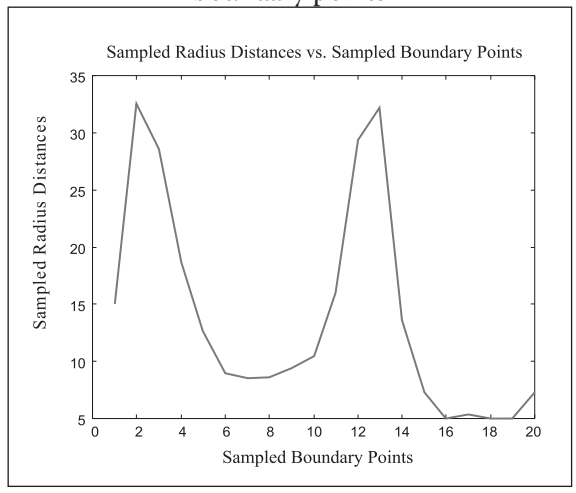

we must ensure that each radius intersects the boundary in only one point. This restriction works for boundaries with concavities which are called "wide convex", like *Salmonella* cells. The optimum N number was determined by performing a one-dimensional Fast Fourier Transform (FFT) on the distances from the centroid to all boundary points. The radius vector number N should be large enough to intersect the boundary at a spatial sampling rate greater than or equal to twice the highest dominant spatial frequency in the boundary spectrum. The smallest *Salmonella* cell could be described by no fewer than N = 20 sampled points. An object with fewer than 20 points would be classified as unknown by the recognition routine. A routine was designed to calculate the distance between the centroid and all the boundary points. A boundary radius vector is created with the radii distances. The coordinates of selected angle values are used to select the corresponding radii from the boundary radius vector.

According to Kashyap and Chellappa.(1981), the $r(k)$ vector can be modeled by a CAR model of the form:

$$r(k) = y(k) + \alpha\,,\ y(k) = \sum_{i=1}^{m} \theta_i y(k-i) + \sqrt{\beta w(k)} \quad (1)$$

where: $r(k)$ = current radius vector length

α = the mean value of $r(k)$

$y(k)$ = zero mean sequence

$\theta_{i,}\ 1 \le i \le m$, = lag coefficients of the zero mean process $y(k)$

$\sqrt{\beta w(k)} = e$ = white noise sequence with variance equal to b

The coefficients $[\theta_{1,\ldots,}\theta_m]$ model the correlated shape variations so that they determine the overall shape of the contour. With the standard least squares method (Draper, 1998), the parameters of the model can be estimated. The solution for the lag coefficients is obtained by first calculating an estimate of α as the mean value of $r(k)$ and subtracting it from $r(k)$ to

Table 1. Training Data Set for *Salmonella* with rod shape (m = 1)

File name	# of Boundary points	a	b	$\alpha/\sqrt{\beta}$	q
St1	36	1.2179	1.8197	0.9028	0.7057
St2	46	1.4836	1.1844	1.3632	0.7513
St3	56	1.8772	4.7695	0.8595	0.6300
St4	52	1.4416	3.5731	0.76793	0.7115
St6	32	1.2617	0.6319	1.5872	0.6720
St14	183	5.0863	36.181	0.8456	0.6869
St15	127	3.8955	16.886	0.94798	0.6925
St19	73	2.1079	3.7684	1.0858	0.7543
St20	81	2.615	6.8763	0.99724	0.7283
St24	165	4.7849	47.662	0.69309	0.6577

obtain the zero mean signal $y(k)$. A complete description of the calculation of the model parameters is described by Trujillo *et. al.* (2001).

Feature Vector Determination

The recognition process assigns class membership to an object by comparing its shape descriptors to the shape descriptors of known objects. In this work, two shape classes for *Salmonella* were defined: rod shape and circle shape (*Salmonella* cell viewed from one end). The labeled shape descriptors correspond to those calculated by our previous routine, i.e., $[\theta,...,\theta_m, \alpha, \beta]$ and describe representative *Salmonella* shapes used as our training set. The training set (Tables 1 and 2) consisted of ten images of individual bacterial cells belonging to each shape class. Special care was taken in the selection of our training images in the sense that all of them had different translation, orientation and size. Based upon the methods described by Dubois and Glanz (1986), the feature vector, ***t***, was chosen to be*: t*= $[\theta_1,...,\theta_m, \alpha/\sqrt{\beta}]$ (2)

Since $\sqrt{\beta}$ is related to the noise of the boundary and a is proportional to the shape size, the parameter $\alpha/\sqrt{\beta}$ can be interpreted as a shape signal-to-noise ratio.

Table 2. Training Data Set for *Salmonella* with circular shape (m = 1)

file name	# of Boundary points	a	b	$\alpha/\sqrt{\beta}$	q
Tcirc1b	34	2.2948	0.4325	3.4894	0.51147
Tcirc2b	29	3.0562	0.2259	6.4296	0.2643
Tcirc3b	32	2.3629	0.3576	3.9513	0.3954
Tcirc4b	44	2.6433	0.1684	6.4411	0.5567
Tcirc5b	30	2.4337	0.2739	4.6950	0.4462
Tcirc6b	45	3.0586	0.1678	7.4668	0.5309
Tcirc7b	40	3.1889	0.1767	7.5855	0.4661
Tcirc8b	26	2.085	0.1924	4.7531	0.4488
Tcirc9b	51	3.9201	0.4147	6.0869	0.4347
Tcirc10b	38	2.8166	0.7357	3.2837	0.4109

Class Shape Discrimination and Decision Rule

Figure 4. Examples of training set pictures

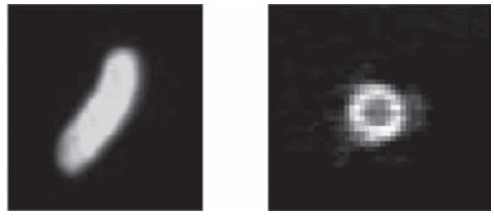

In Figure 4 the two class shapes are presented. All shapes are convex or wide-sense convex and have their centroids inside and relatively far from the boundary. The feature weighting (FW), a minimum distance classifier, was described in detail in a previous research (Trujillo *et. al.*, 2001). In summary, the FW technique detects the feature most common to the training set samples and emphasizes that feature in classifying an unlabeled sample. An unlabeled sample was classified by assigning it to the class whose cluster of sample points was closest in the weighted mean square distance sense. The decision rule, which mathematically describes the pattern space partitions, was formed by the classifier training procedure.

In this work, a modified version of the FW method, with rotated coordinates (FWR), was implemented to compare performances. In the FW method, the weights were inversely proportional to the feature standard deviations in the direction of the original coordinate axes. In the FWR method, the class transformations are expanded to allow a rotation of the coordinate system, as well as scaling of the rotated coordinate system axes. According to Dubois and Glanz (1986), the rotated coordinate system recognition scheme, which forms decision boundaries at the intersection of rotated ellipsoidal contours of constant mean-square distance from the training samples of each class, place greater emphasis on intra-class similarities than the mean-square intra-class distance in the weighted only pattern space. The feature weights that minimize the intra-class distance in the rotated coordinate method are:

$$w'_{ii} = \left(\prod_{j=1}^{m+1}\sqrt{\lambda}_j\right)^{1/(m+1)}(1/\sqrt{\lambda}_i),\ i=1,...,m+1, \text{ and } j=1,...,3 \quad (3)$$

where $\sqrt{\lambda_j} = \sigma_j'$ is the sample standard deviation in the direction of the j[th] sample covariance matrix eigenvector. The covariance matrix (*CM*) is estimated from the two sample vectors of the class training sets described previously and has the form:

$$CM = \sum_{i=1}^{m+1}\sum_{k=1}^{m+1} \overline{p_i p_k} - \overline{p}_i \overline{p}_k \quad (4)$$

The eigenvectors $\boldsymbol{U}$ and eigenvalues $\boldsymbol{l}$ of the sample covariance matrix were calculated using the MATLAB function [$\boldsymbol{U}$, $\boldsymbol{l}$] = ***eig***(CM). The feature weighting distance equation for the FWR method is similar to the FW equation but with the difference that, the weights and sample points were expressed in terms of the rotated coordinate system. The distance, $d(\boldsymbol{g}', \boldsymbol{C}')$, between an unlabeled vector $\boldsymbol{g}$ and the cluster of L samples of class C is:

$$d(g', C_L') = \sum_{i=1}^{m+1} w'^2{}_i \left[(g'_{i-} \overline{C}'_i)^2 + \sigma'^2{}_i\right] \quad (5)$$

where:

$\overline{C}'_i$ = is the sample mean vector of the i^{th} feature expressed in rotated coordinates.

σ'^2_i = is the sample variance in the direction of the j[th] sample covariance matrix eigenvector.

Any vector, for instance the unlabeled vector $g = [g_1 \quad g_2]$ expressed in original coordinates, can be expressed in rotated coordinates by the transformation:

$$g' = U^T g = \begin{bmatrix} u_1^T \\ u_2^T \end{bmatrix} g \,, \quad (6)$$

where u_1 and u_2 are eigenvectors of *CM.*

Notice that the i[th] feature weight is inversely proportional to the standard deviation of the i[th] training set feature expressed in rotated coordinates. Each eigenvalue, l_i, is the variance of the feature points in the direction of the i[th] eigenvector. An unlabeled sample is most heavily set by its similarity to the class mean feature in the direction of the eigenvector with the smallest eigenvalue. The classifier is trained on each class by calculating the sample covariance matrix and the corresponding eigenvectors and eigenvalues, and calculating the weights and sample mean of each feature of a class training set. For each class, covariance matrices, eigenvectors, eigenvalues, weights, and sample means are stored in vector form. The sample mean vectors and the unlabeled sample are transformed to the rotated coordinates, and the equation (5) is calculated. The decision rule assigns the unlabeled shape to the class corresponding to the smallest distance.

In addition to shape discrimination, size restrictions were applied for the cases in which unknown objects (i.e., debris) resembled rods or circles. As reported by Trujillo *et. al.*, (2001), any object with a number of boundary points less than 20 or more than 190 was labeled as unknown. In order to refine shape discrimination, a new restriction was applied to enhance the recognition of circular bacteria: Based on data shown in Table 3, any circular shape with radius distances smaller than 1.3 and bigger than 3.6 was also labeled as unknown.

Table 3. Difference Between Maximum and Minimum Radius Distances For Class 2 Training Set.

File Name	Maximun	Minimun	Difference
Tcirc1	5.831	3.162	2.669
Tcirc2	5.000	3.162	1.838
Tcirc3	5.000	3.000	2.000
Tcirc4	6.403	5.000	1.403
Tcirc5	5.385	3.162	2.223
Tcirc6	7.280	5.385	1.895
Tcirc7	6.403	5.000	1.403
Tcirc8	5.000	3.000	2.000
Tcirc9	8.544	5.000	3.544
Tcirc10	6.324	3.162	3.162

Shape discrimination capabilities of the CAR model parameters

In order to study the shape discrimination capabilities of the CAR model parameters, recognition experiments were performed on four slide samples containing *Salmonella typhimurium* from chicken carcass wash water (one extra slide without *Salmonella* was used as a control). From each slide, 25 pictures were acquired and recorded applying the multi-plane focus techni-

que (Trujillo et. al., 2001). The location for the pictures was selected randomly and within the area of the polycarbonate membrane. The polycarbonate membrane had an effective area of 78.54 mm^2 and the area of each field of view was 0.002884 mm^2 (0.0465 mm x 0.062 mm). According to previous calculations, there were 27,233 fields of view for each sample slide. Finally, the results corresponding to recognition of the composite images by the computer-based system, were compared with the manual counting of the same images by a trained bacteriologist. The *Salmonella* cells were counted in images displayed on the computer monitor. No restriction in time was established for the manual counting to minimize the errors produced by human fatigue. It was imperative to compare the automated recognition and enumeration results against human performance in full capacity. An example of the output produced by the computer is shown in Figure 5.

Figure 5. Example of Automatic Recognition/Enumeration

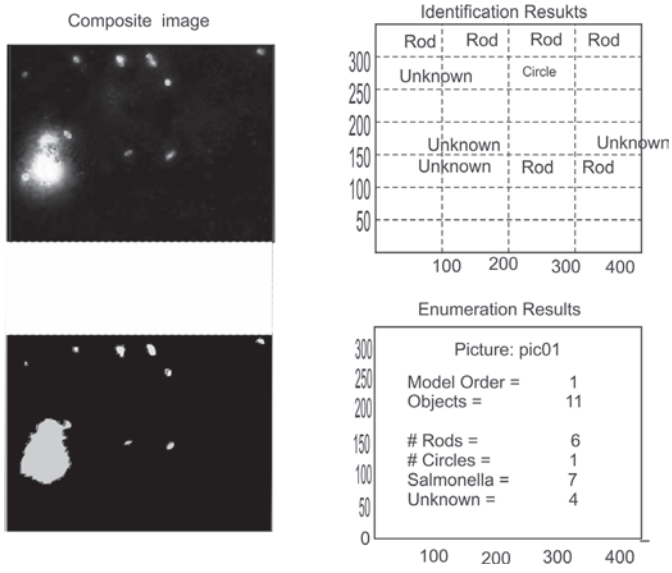

Results and discussion

Table 4 shows the results of the calculation of sample means, sample variances, and weights for both the FW and FWR methods. For each class shape, the covariance matrices and the corresponding eigenvectors and eigenvalues used by the FWR method are shown in Table 5. A comparison of the results obtained by the computer-based system before and after the introduction of the FWR method and circular size restrictions can be seen in Table 6. The modifications pro-

Table 4. Sample Means, Variances and Weights determined using both FW and FWR Methods

Class/ Feature		FW Method *Mean Variance Weights*			FWR Method *Mean Variance Weights*		
Rod	θ	6.9903e-1	1.5809e-3	2.6366e+0	-6.5552e-1	1.2999e-3	2.6981e+0
	α/√β	1.0050e+0	7.6402e-2	3.7928e-1	1.0339e+0	6.8883e-2	3.7063e-1
Circle	θ	4.4656e-1	6.7875e-3	4.3988e+0	-4.0853e-1	5.9962e-3	4.4194e+0
	α/√β	5.4137e+0	2.5412e+0	2.2733e-1	5.4167e+0	2.2873e+0	2.2628e-1

Table 5. Covariance Matrix, Eigenvectors, And Eigenvalues For Each Class Shape

Class	FWR Method *Covariance Matrix*	*Eigenvectors*	*Eigenvalues*
Rod	$\begin{bmatrix} 1.4229e-3 & 2.8807e-3 \\ 2.8807e-3 & 6.8760e-2 \end{bmatrix}$	$\begin{bmatrix} -9.9909e-1 & 4.2663e-2 \\ 4.2663e-2 & 9.9909e-1 \end{bmatrix}$	1.2999e-003 6.8883e-002
Circle	$\begin{bmatrix} 6.1086e-3 & 1.6018e-2 \\ 1.6018e-2 & 2.2872e+0 \end{bmatrix}$	$\begin{bmatrix} -9.9998e-1 & 7.0217e-3 \\ 7.0217e-3 & 9.9998e-1 \end{bmatrix}$	5.9962e-003 2.2873e+000

duced a count reduction in both rods and circles but relatively in the same proportion.

The size restriction for circular shapes produced significant changes in the all counts. Fifty seven objects, which were classified mostly as circles before the modifications, were classified as unknowns after the modifications. The increase of 13 objects was due to the reduction of one erosion step in the disconnect algorithm described in previous report (Trujillo, *et. al*., 2001). These 13 objects were classified as unknown for having less than 20 boundary points.

Table 6. Comparison of Total Counts of Objects, Class Shapes, Bacterial Cells, and Unknown Objects Detected by Computer Before and After Improvements

Method	Objects	Rods	Circles	Cells	Unknowns
Before	1003	607	206	813	190
After	1016	598	158	756	260

In general, no bacterial cells were found in either the control slide or slides with bacterial concentrations below 10^4 CFU/ml. Given the size of the scanning area (27,000 fields of view), and low concentrations, the probability of getting false negatives was significant. A similar result was reported by Huang *et al.* (1999) who estimated the real number *of Salmonella typhimurium* in 110 samples and prepared them under almost the same conditions reported in this study. Table 7 shows the results from both automatic methods and manual counting. The difference between manual counts and automatic counting with previous results was approximately 7%. After the improvements, the difference was reduced to less than 1%, based upon over 100 images of four specimen slides. The FWR method produced a reduction in the absolute error of approximately 50% for slides 2 and 3. In slides 1 and 4 the absolute error increased and decreased respectively but almost in the same proportion.

The computer-based system took about 2 h to process the samples, including the time of sample preparation (1 h), imaging equipment set up (5 min), data collection (30 min with both multi-plane and XY scanning), multi-plane algorithm (6 s per field of view), and recognition/enumeration (5 s per field of view). The bacteriologist spent an average of 1 min to analyze each image manually for a total of 1 h and 40 min. Comparing with other reported investigations (Singh, *et al.*, 1997 and Huang, *et al.*, 1999) the time needed by our system is approximately 40 min less because they did not take advantages of the implementation of a multi-plane focus scanning (Trujillo, *et. al*., 2001). However, the system speed could be improved if a faster computer were used.

Conclusions

This investigation indicates that a microscope-based machine vision system that can recognize and enumerate *Salmonella typhimurium* is feasible. The CAR model parameters showed valuable properties in differentiating the two-shape classes characteristic of *Salmonella* cells: the rod shape and the circular shape. Specifically, the two model parameters, θ and $\alpha/\sqrt{\beta}$, presented consistent intra-class similarities for each model order and reduced inter-class resemblance. The introduction of both the feature weighting and the circular size restriction reduced the differences between automated enumeration and manual counting. The accuracy of the system is comparable to a bacteriologist's performance and faster than human counting (without taking human fatigue in account). Advantages of the system are that it was rapid and simple, cell morphology could be assessed, and direct microscope counts could be recorded. In addition, the speed could be increased using a faster computer. Since the results can be determined in approximately 2 h, this system might be suitable for rapid screening of *Salmonella* by the poultry industry.

Acknowledgements

The authors thank Awilda O'Leary for her technical assistance.

References

Chen, Z.D., Chang, R.F. and Kuo, W.J. 1999. Correspondence - Adaptive Predictive Multiplicative Autoregressive Model for Medical Image

Compression. *IEEE Transactions on Medical Imaging*, 18(2):181-184.

Draper, S. 1998. *Applied Regression Analysis*. New York: John Wiley & Sons.

Dubois, S. R. and Glanz, F. H., 1986. An Autoregressive Model Approach to Two- Dimensional Shape Classification. *IEEE Transactions On Pattern Analysis And Machine Intelligence*, 8(1):55-65.

Ghazanfari, A. and Irudayaraj, J. 1996. Classification of Pistachio Nuts Using a String Matching Technique. *ASAE* 39(30:1197-1202.

Hand, A. and McCarthy, D., eds. 2000. Interactive Story: From Corn to Cupcakes. *Photonics Spectra*, 34(3):91-103.

Huang, J., Li. Y., Slavik, M.F., Bayyari, G. and Tao, Y. 1999. Identification and Enumeration of *Salmonella* on Sample Slides of Poultry Carcass Wash Water Using Image Analysis*. Transactions of the ASAE*, 42(1):267-273.

Kashyap, R.L. and Chellappa, R. 1981. Stochastic Models for Closed Boundary Analysis: Representation and Reconstruction. *IEEE Transaction on Info Theory*, 27(5):627-637.

Paulik, M., Das, M., and Loh, N.K. 1992. Nonstationary Autoregressive Modeling of Object Contours. *IEEE Transactions On Signal Processing*, 40(3):660-675.

Pratt, W. K. 1991. *Digital Image Processing*, pp. 623-625. New York: John Wiley & Sons.

Singh, N., Slavik, M, Wang, X. and Li, Y., 1997. Image Analysis as a Rapid Pathogen Detection Method for Use in Poultry Industry. *Journal of Rapid Methods and Automation in Microbiology*. 5:205-214.

Trujillo, O. 2000. Bioimaging Analysis for rapid Recognition of Pathogens on Poultry Materials. MS Thesis: University of Arkansas, Fayetteville.

Trujillo, O., Griffis, C., Li, Y., and Slavik, M. 2001. A Machine Vision System Using Immuno-Fluorescence Microscopy For Rapid Recognition of *Salmonella typhimurium*. *Journal of Rapid Methods and Automation in Microscopy*. 9:115 -134.